Fermi National Accelerator Laboratory

FERMILAB-Pub-95/220-A

Condensation of Bosons in Kinetic Regime

D.V. Semikoz and I.I. Tkachev

Fermi National Accelerator Laboratory
P.O. Box 500, Batavia, Illinois 60510

Operated by Universities Research Association Inc. under Contract No. DE-AC02-76CHO3000 with the United States Department of Energy

Disclaimer

This report was prepared as an account of work sponsored by an agency of the United States Government. Neither the United States Government nor any agency thereof, nor any of their employees, makes any warranty, expressed or implied, or assumes any legal liability or responsibility for the accuracy, completeness, or usefulness of any information, apparatus, product, or process disclosed, or represents that its use would not infringe privately owned rights. Reference herein to any specific commercial product, process, or service by trade name, trademark, manufacturer, or otherwise, does not necessarily constitute or imply its endorsement, recommendation, or favoring by the United States Government or any agency thereof. The views and opinions of authors expressed herein do not necessarily state or reflect those of the United States Government or any agency thereof.

FERMILAB-Pub-95/220-A

Condensation of bosons in kinetic regime

D. V. Semikoz[1] and I. I. Tkachev[1,2]

[1] *Institute for Nuclear Research of Russian Academy of Sciences, Moscow 117312, Russia*

[2] *NASA/Fermilab Astrophysics Center Fermi National Accelerator Laboratory, Batavia, IL 60510*

(September 20, 1995)

hep-ph/9507306 14 Jul 95

Abstract

We study the kinetic regime of the Bose-condensation of scalar particles with weak $\lambda\phi^4$ self-interaction. The Boltzmann equation is solved numerically. We consider two kinetic stages. At the first stage the condensate is still absent but there is a nonzero inflow of particles towards $\mathbf{p} = \mathbf{0}$ and the distribution function at $\mathbf{p} = \mathbf{0}$ grows from finite values to infinity in a finite time. We observe a profound similarity between Bose-condensation and Kolmogorov turbulence. At the second stage there are two components, the condensate and particles, reaching their equilibrium values. We show that the evolution in both stages proceeds in a self-similar way and find the time needed for condensation. We do not consider a phase transition from the first stage to the second. Condensation of self-interacting bosons is compared to the condensation driven by interaction with a cold gas of fermions; the latter turns out to be self-similar too. Exploiting the self-similarity we obtain a number of analytical results in all cases.

PACS numbers: 05.30.Jp, 32.80.Pj, 95.35.+d

Typeset using REVTEX

I. INTRODUCTION

It is a fundamental result of quantum statistics that above a certain critical density all added bosons must enter the ground state: a Bose-Einstein condensate (BEC) forms. Gas of weakly interacting bosons allows a well-defined theoretical microscopic treatment of this process. However, Bose condensation has not yet been observed in a real physical system which could be described as an ideal gas. Superfluid ^{4}He, for example, is a system with very strong interaction and is considered as a quantum liquid.

One can reach Bose condensation by gradually decreasing the temperature in a sequence of equilibrium states. An appropriate description of this regime is given by the well-known theory of second order phase transitions [1]. On the other hand, the conditions for the formation of a Bose condensate can appear when the system is far from equilibrium. This will be generally true for the condensation of an ideal gas because of the weakness of interaction. The kinetics of Bose-condensation in this case is an important and interesting problem.

Recently this subject has attracted particular interest in connection with the exciting prospects for experimental observation of a Bose condensation in very cold atomic samples, *e.g.* in a gas of spin-polarized atomic hydrogen [2, 3] or in alkali-metal vapors [4], as well as in the gas of excitons (bound states of electrons and holes in semiconductors) [5]. For instance, Doyle *et. al.* [3] report to have attained $n \approx 10^{14}$ cm^{-3} and $T \approx 100$ μK, which is only a factor of 3 above the temperature of Bose condensation at this density.

Since the life-time of a sample in all experiments is finite and short, the question of a time-scale for the formation of Bose-condensate is a central one.

Another interesting application of Bose kinetics is rather far from laboratory experiments and is related to the problem of Bose star [6] formation [7] from the dark matter in the Universe. The life-time of the "sample" is not limited in this case, but in the only model [8] for Bose-star formation which involves a realistic dark matter particle candidate, the axion [9], the self-interaction of particles is so weak that the relaxation time is comparable to the age of the Universe. The possibility of Bose-star formation becomes dependent upon the exact value of this time-scale.

In experiments with atomic hydrogen or with alkali-metal vapors the Bose-gas is effectively isolated from its surroundings and the relaxation to thermal equilibrium and condensation is expected to occur due to particles' self-coupling only. The same is true for the case of axion miniclusters. On the contrary, interaction with the thermal heat bath is important in the dynamics of excitons. We consider both situations in the present paper. However, we only consider the simplest $\lambda\phi^4$ self-interaction of structureless scalar particles (this approximation is exact *e.g.* in the axion case). The heat bath is modelled by a gas of heavy fermions.

The process of Bose condensation can be divided into three stages. The first and the third ones are kinetic stages which occur before and after actual nucleation of the condensate. These two stages can be treated with the Boltzmann equation which describes restructuring of the distribution function at the first stage and growth of the condensate at the third. A numerical study of these two stages is the purpose of the present paper (we have reported the main results in Ref. [10]).

In the framework of the kinetic equation there is no condensate at all times if there was

no condensate initially. Therefore we have to add a small seed condensate "by hand" in this framework when switching from the first to the third stages. We switch between stages when the distribution function becomes infinite at zero momentum. We do not consider the second stage, *i.e.* how the condensate actually emerges, which is, in fact, a phase transition. A description of the second stage has been elaborated in Ref. [11]. Since the duration of this stage is short and the magnitude of the condensate which appears is small [11], our approach seems to be reasonable.

The question of the time evolution of a weakly interacting Bose gas during the first kinetic stage was addressed in a number of papers. In earlier treatments an ideal Bose gas was coupled to a thermal bath with infinite heat capacity: to a phonon bath in Ref. [12] and to a fermi heat bath in Ref. [13]. A small energy exchange was assumed and after several other approximations a Fokker-Planck type of equation was obtained. Levich and Yahkot [13] calculated analytically that the time for condensation (more precisely, the time needed for the distribution function to reach infinity at zero momentum) is infinite in this situation. By including boson-boson interactions they later [14] found a solution which describes the explosive emergence of a condensate, but they concluded that this effect could have been an artifact of their approximations.

Snoke and Wolfe in Ref. [15] undertook a direct numerical integration of the Boltzmann kinetic equation. Although this calculation demonstrated a restructuring of the distribution of particles, the appearance of a Bose condensate (more precisely, an infinite value of the distribution function at zero momentum) was not detected. As compared with Ref. [15], we carry out the numerical integration in a much wider dynamical range of relative energies and densities. The major and important difference of our approach is that we directly analyse the behavior of the distribution function, while Snoke and Wolfe considered an integrated quantity $n(\varepsilon)$, the number of particles with the energy less than a given value ε.

Analytical study of Bose condensation was performed recently by Kagan, Svistunov and Shlyapnikov in the paper [16] where three different regimes of evolution were identified and considered. Our numerical results confirm qualitative predictions of that work. In particular, it was argued that in the kinetic region of the non-linear regime the distribution function has the form $f(\varepsilon) \sim \varepsilon^{-7/6}$ for small ε. We indeed observe the tendency to this law in our numerical integration, but, while being close to it, the system never reaches this critical exponent. Instead of $7/6 \approx 1.17$ we obtain 1.24. Moreover, this distribution is destroyed when the condensate emerges, the fact that was not stressed in Ref.[16]. As concerns the condensation time, only order of magnitude dimensional estimates were obtained in Refs. [7, 16].

We find that during the first kinetic stage the distribution function became infinite at zero momentum in a finite time in the case of self-interacting bosons. This stage can be divided into two parts. During the first part of the first stage the distribution function is restructured so that a self-similar solution is formed; the distribution function does not grow much during this time interval which takes about half of the entire evolution time. During the second part, the distribution function rapidly (as a pole power law $\propto (t_c - t)^{-2.6}$) reaches infinity at $\mathbf{p} = 0$ in a self-similar way.

Despite the fact that the Bose-condensation is inherently based on Bose-statistics, the kinetics of this stage is a classical process and not a quantum one. To be precise, it corresponds to the kinetics of classical waves (but not classical particles). Actually, the equations

we encounter here and the resulting behavior of the system are well-known in the theory of turbulence [17, 21, 23]. This is no wonder. Indeed, a Bose condensation occurs when the occupation numbers are large, $f(\mathbf{p}) \gg 1$. In that case we can replace quantum creation operators by amplitudes of classical waves. The corresponding kinetic equation can be obtained in two ways: either neglecting 1 in the product of all factors $[1 + f(\mathbf{p_i})]$ in the quantum kinetic equation (by which we neglect the spontaneous scattering with respect to the induced one), or directly in the random phase approximation for the ensemble of classical waves [21, 23]. The second approach is customary in the theory of turbulence, but the result is the same in both approaches.[1] While it may be more appropriate in the second approach to refer to $f(\varepsilon)$ as a density of waves in phase space, we will continue to call it density of particles in phase space.

The power law behavior of the distribution function we observe, with an exponent close to 7/6, is a special case of the Kolmogorov turbulence [18, 19, 20]. Indeed, by definition, turbulence is a stationary state characterized by a non-zero flow (in phase space) of some conserved quantity. In the case of Bose-condensation we have a flux of particles towards the condensate, which tends to be constant across the energy space, and this corresponds to $f(\varepsilon) \propto \varepsilon^{-7/6}$. An explosive behavior of the distribution function at $\mathbf{p} = 0$ which we observe was also found in other instances of turbulence [22, 23].

The actual nucleation of the condensate cannot be described in the framework of the kinetic equation. But we have to conclude that after the distribution function has become infinite at zero momentum, the condensate forms. Kinetic equations which describe the third stage in the presence of the condensate were derived in Refs. [24]. We re-derive those equations in a simpler way which is valid when the difference between particles and quasiparticles is unimportant. We consider this weak coupling regime only. We found that during the third stage the evolution is also self-similar until the restructuring in the phase-space reaches the tail of the distribution.

We compare this condensation process, which is due to self-interaction of particles, to the condensation driven by the interaction with a cold bath, for which we also solved the Boltzmann equation numerically. We find that the distribution function grows with time only as $\propto t^3$ in this case. The energy dependence of the distribution function is also different now. Instead of a singular power law profile, $f(\varepsilon) \sim \varepsilon^{-7/6}$, which corresponded to the constant flux of particles towards the condensate, now all excess particles form a well defined packet in the momentum space. The total number of particles in this packet remains constant during the evolution, while its width decreases, gradually approaching a δ-function [13]. This type of behavior is qualitatively different from the one we have in the case of self-interacting bosons. However, it is also self-similar and one of the predictions of the self-similarity in this case is that $f(\varepsilon = 0, t) \propto t^3$. In general, using the properties of the self-similarity enables us to obtain a number of analytical results, *e.g.* the relation of the critical exponent β in $f(\varepsilon = 0, t) \propto (t_c - t)^{-\beta}$ to the critical exponent α in $f(\varepsilon) \propto \varepsilon^{-\alpha}$.

The fact that the system interacting with a cold bath needs infinite time (in the kinetic

[1] This is particularly important for the axion case, because axions in miniclusters [8] are from the very beginning in a state of gravitationally bounded classical waves and one may wonder (or be suspicious of) how Bose-condensation could occur in such a system.

framework) to reach infinity in the distribution function at $\mathbf{p} = 0$ does not necessarily mean that the condensation time is infinite for this system. Indeed, the nucleation of the condensate is a phase transition which does not have to occur at the moment when the distribution reaches infinity, and can occur earlier.

Although our prime interest and motivation for this work were connected with the physics of Bose stars, the problem of condensate formation in a gravitational field has never been considered, and we do not consider it here. Instead, we are solving kinetic equations in flat space-time and only the range of parameters of the initial distribution can reflect the virial equilibrium of a self-gravitating system.

When this work was completed B. Svistunov brought to our attention his paper [25]. He also analyzed two non-linear kinetic stages exploiting the assumption of self-similarity. His approach is close to ours and our results qualitatively confirm the results and predictions of Ref. [25]. However, he assumed a priory in his analysis that the critical exponent is $\alpha = 7/6$. He concluded that this assumption had passed his numerical self-consistency check, but we believe that this is due to the fact that he used energy grid with the minimum value $\varepsilon_{\min} = 10^{-3}$, while in our case it was $\varepsilon_{\min} = 10^{-9}$.

The plan of this work is as follows. In Sec. II we reduce the Boltzmann kinetic equation to the form suitable for numerical integration, both in the absence and presence of the condensate. In Sec. III we present the results of numerical integration which describe the evolution of one-particle distribution function in the case of self-interacting bosons, while Sec. IV is devoted to the evolution of a Bose system interacting with fermion bath of infinite heat capacity. In Sec. V we derive analytical consequences of self-similar behavior of the distribution function. In the final section VI we discuss some possible applications and present conclusions. Appendix A describes an analytical reduction of the collision integral. In Appendix B the static ("turbulent") power law solutions to the kinetic equation are described. Appendix C is a technical supplement to Sec. IV.

II. THE KINETIC EQUATION

In a state of thermal equilibrium any system of bosons has to have the Bose-Einstein distribution of particles over the energies. In order to reach this state particles need to interact either with the thermal bath of other particles or with each other. We shall consider both cases: the system of scalar bosons with 4-particle self-interaction and an ideal Bose gas coupled to cold gas of fermions. The time development of a state which contains large number of particles can be adequately described by the kinetic equation which governs the evolution of the one-particle distribution function, $f(\mathbf{p})$. The only process which contributes to the Boltzmann kinetic equation is illustrated in Fig. 1 for each case we consider, and the equation takes the form:

$$\frac{df(\mathbf{p}_1)}{dt} = \frac{(2\pi)^4}{2p_{01}} \int \delta^4(\sum_k p_{\mu k}) |M_{fi}|^2 F(f) \prod_{k=2}^{4} \frac{d^3\mathbf{p}_k}{(2\pi)^3 2p_{0k}}\,, \tag{2.1}$$

where $(p_{0k}, \mathbf{p}_k)$ are components of the four-vector $p_{\mu k}$. For the conceptual convenience we wrote this equation in the most general Lorentz-invariant form, but in what follows we shall

consider only the non-relativistic limit of it. For the quartic self-interaction, Fig. 1a, we have

$$F(f) = [1+f_1][1+f_2]f_1'f_2' - [1+f_1'][1+f_2']f_1f_2, \tag{2.2a}$$

where $f_k \equiv f(\mathbf{p}_k)$, $f_k' \equiv f(\mathbf{p}_k{}')$ (we assume the convention $1' = 3$, $2' = 4$), while for the interaction with the fermion bath, Fig 1b :

$$F(f) = [1+f_1][1-\eta_2]f_1'\eta_2' - [1+f_1'][1-\eta_2']f_1\eta_2, \tag{2.2b}$$

where $\eta_k \equiv \eta(\mathbf{p}_k)$ is the one particle distribution function of fermions which we shall not evolve here and consider it to be fixed to the equilibrium.

The field-theoretical Lagrangian which we bear in mind for the case of self-interacting bosons is

$$\mathcal{L} = \frac{1}{2}\partial_\mu\phi^2 + \frac{m^2}{2}\phi^2 + \lambda\frac{\phi^4}{4!} \ . \tag{2.3}$$

and the corresponding matrix element is given by

$$|M_{fi}|^2 = \lambda^2 \ . \tag{2.4}$$

The matrix element of the process in Fig. 1b in the non-relativistic limit is also momentum independent, $|M_{fi}|^2 = g^4$.

The Bose-Einstein distribution function is

$$f(\mathbf{p}) = \frac{1}{\exp\left[(\varepsilon-\mu)/T\right]-1} + (2\pi)^3 n_c \delta(\mathbf{p}) \ , \tag{2.5}$$

where ε is the particle energy, μ is the chemical potential, T is the temperature of the final state and n_c is the density of particles in the condensate. The fact that distribution function (2.5) is a solution to the equation $df(\mathbf{p}_1)/dt \equiv I_{\rm coll}(\mathbf{p}_1) = 0$ is a simple consequence of the energy-momentum conservation in each particle interaction vertex and does not depend upon the specific form of the matrix element M_{fi}.

One expects that an arbitrary initial distribution function $f(\mathbf{p})$ will evolve via equation (2.1) to its static solution (2.5) just because the static solution can not evolve any further.[2] This implies that simple and straightforward numerical iteration procedure has to be robust. Given the distribution function at time t we calculate the collision integral and then we advance the distribution function in time as $f(\mathbf{p}, t+\Delta t) = f(\mathbf{p}, t) + I_{\rm coll}(\mathbf{p}, t)\Delta t$.

The evolution of the initial distribution function which allows for the condensate formation consists of two stages. In the first stage condensate is absent and the distribution function is finite. In the second stage $n_c \neq 0$ and the distribution function has δ-function singularity. Consequently, we have to derive the kinetic equation in the form suitable for the numerical integration in each of those cases separately.

---

[2] The situation is not that simple, however, since the kinetic equation at $f \gg 1$ has many static solutions, and our system first tend to evolve to the turbulent distribution, see Appendix B, and would stay there (which it does in our numerical experiments) if the phase transition with a nucleation of the condensate would not occur.

A. Zero initial condensate

In what follows we shall consider an isotropic initial distribution $f = f(\varepsilon)$ and the non-relativistic limit $\varepsilon = \mathbf{p}^2/2m$. The kinetic equation for the case without condensate, $n_c = 0$, can be rewritten in the form (see Appendix A):

$$\frac{df(\varepsilon_1)}{dt} = \frac{|M_{fi}|^2}{64\pi^3 m} \int\int F(f) \frac{D}{p_1} d\varepsilon_1' d\varepsilon_2' \equiv I_{\rm P} \ , \tag{2.6}$$

where

$$D \equiv \min[p_1, p_2, p_1', p_2'] \ . \tag{2.7}$$

The integration should be done over the white area of Fig. 2 which is divided into four regions. In each of those regions we have

$D = p_2$ in I region	$D = p_1$ in II region
$D = p_2'$ in III region	$D = p_1'$ in IV region

In the argument of $F(f)$ according to the conservation of energy $\varepsilon_2 = \varepsilon_1' + \varepsilon_2' - \varepsilon_1$.

It is possible [19], to map regions II-IV in Fig. 2 to the region I , and then to rewrite the collision integral in Eq. (2.6) as an integral over the region I only. This representation is essential in finding the stationary solutions to Eq. (2.6) [19] and the corresponding Kolmogorov's spectra, see Appendix B 1.

B. Non-zero condensate

This case we shall consider for bosons with self-interaction only. After the moment of condensate formation the kinetic equation (2.6) is inappropriate for numerical integration, and the finite number of particles in the condensate corresponds to the infinite value of the distribution function at zero energy. In order to describe the system of particles interacting with the condensate we divide the distribution function into two pieces:

$$\tilde{f} = f(\varepsilon, t) + (2\pi)^3 n_c(t) \delta^3(\mathbf{p}) \ , \tag{2.8}$$

where the first term corresponds to the "gas" of particles and the second one describes the condensate. Substituting this function into the original kinetic equation (2.1) we obtain

$$\dot{n_c}(t) = \frac{\lambda^2 n_c(t)}{64\pi^3 m} \int_0^\infty d\varepsilon_1' d\varepsilon_2' [f_1' f_2' - f_2(1 + f_1' + f_2')] \ , \tag{2.9a}$$

$$\dot{f}(\varepsilon_1) = I_P + \frac{n_c(t)\lambda^2}{32\pi m^2 p_1} \left(\int_0^{\varepsilon_1} [f_1' f_2' - f_1(1 + f_1' + f_2')] d\varepsilon_2' + 2 \int_{\varepsilon_1}^\infty [f_2'(1 + f_1 + f_2) - f_1 f_2] d\varepsilon_2' \right) \ . \tag{2.9b}$$

In Eq. (2.9b) $\varepsilon_1' = \varepsilon_1 - \varepsilon_2'$ and $\varepsilon_2 = \varepsilon_2' - \varepsilon_1$, while in Eq. (2.9a) $\varepsilon_2 = \varepsilon_1' + \varepsilon_2'$.

In general, after the condensate formation (and at large particle densities even before) the description in terms of quasiparticles rather then particles is more appropriate. For example, the kinetic equation (2.9) does not include the processes where one of the incoming and one of the outgoing particles have zero momentum, $p_2' = p_2 = 0$. This process does not contribute to the collision integral directly; *i.e.*, it does not change the distribution of particles over energies, but it does change the effective particle mass. However, in many cases those effects are insignificant and we still can work in terms of particles. Quantitatively, the original particle picture is correct if the potential energy contribution from the interaction with the condensate to the effective particle mass squared, $\Delta m_{\rm eff}^2 = \lambda\phi_c^2/6 = \lambda n/m$, is smaller than the particle momentum squared, *i.e.* $\lambda n/m \ll p^2$. In fact, the kinetic equations of Refs. [24] which contains all quasiparticle effects do coincide in this limit with our Eq. (2.9) derived in a simple way. Since $n \sim m^3(\Delta v)^3 f_0$, we obtain $\lambda f_0(\Delta v) \ll 1$ as a condition of validity of our equations, where Δv is the characteristic velocity dispersion. In the case of axion miniclusters, for example, we have [8] $\lambda f_0 \sim 10^{-5}$; $\Delta v \sim 10^{-8}$, and the description in terms of particles is perfectly good.

Note also that the kinetic equation itself becomes invalid at characteristic energies smaller than the inverse relaxation time, but this condition is always weaker than the previous one.

III. SELF-INTERACTING BOSONS

A. Initial distribution and the rescaling of time

Let us first consider the system of self-interacting bosons. As an initial distribution we choose the function $f(\varepsilon)$, which has a maximum at $\mathbf{p} = 0$. In general, such a distribution function can be characterized by means of three major parameters:

(1) The overall amplitude f_0. In what follows we define $f_0 \equiv f(\varepsilon = 0)$.

(2) The energy scale ε_0, where the distribution function becomes 2 times smaller, $f(\varepsilon_0) = f_0/2$.

(3) The effective width Γ of the region over which the distribution function varies rapidly.

More specifically, we choose the initial distribution function to be of the form:

$$f(\varepsilon) = \frac{2f_0}{\pi} \arctan\left[\exp\left(\Gamma(1 - \varepsilon/\varepsilon_0)\right)\right] . \tag{3.1}$$

In what follows we shall measure the distribution function in units of f_0, *i.e.* the initial distribution function which will appear throughout the rest of this section will have the normalization $f(\varepsilon = 0) = 1$, and we shall measure the energy in units of ε_0.

We define the dimensionless time τ as [7]

$$\tau = \frac{\varepsilon_0^2 f_0(1 + f_0)\lambda^2}{64\pi^3 m}\, t . \tag{3.2}$$

The parameter ε_0 after rescaling will not enter the kinetic equation explicitly, but will define the time scale of the evolution. The parameter f_0 defines the time scale as well, but it remains present in the equation through the definition of F if $f_0 \sim 1$:

$$F(f) = \frac{f_1' f_2' - f_1 f_2 + f_0([f_1 + f_2] f_1' f_2' - [f_1' + f_2'] f_1 f_2)}{1 + f_0}. \tag{3.3}$$

Otherwise it also disappears from the rescaled equation: in the limit $f_0 \ll 1$ one can neglect terms $\sim f^3$, and in the limit $f_0 \gg 1$ it is possible to drop terms $\sim f^2$ in Eq.(3.3)

In terms of τ there remains the weak dependence of the relaxation time upon the initial shape parameter Γ. All data presented in this section will correspond to one and the same value of $\Gamma = 5$.

After rescaling everything in Eq.(2.6) is of order unity and, very roughly, it is expected that the time-scale of the relaxation towards the equilibrium corresponds to $\tau \sim 1$, see Ref.[7].

While the distribution function Eq.(2.5) has three characteristic parameters $\{T, \mu, n_c\}$, only two of them are non-zero simultaneously. Those two non-zero parameters are uniquely defined by the values of two conserved quantities: densities of the energy and the number of particles:

$$e = \int \varepsilon f(\mathbf{p}) \frac{d^3\mathbf{p}}{(2\pi)^3} \ , \tag{3.4a}$$

$$n = \int f(\mathbf{p}) \frac{d^3\mathbf{p}}{(2\pi)^3} \ . \tag{3.4b}$$

With the shape of the initial distribution function being given, the two scaling parameters f_0 and ε_0 in addition to fixing the time scale define also the parameters of final equilibrium $\{T, \mu, n_c\}$. This correspondence is illustrated in Fig. 3.

The solid curve divide the plane of Fig. 3 in two regions and corresponds to the equilibrium distribution function with $\mu = n_c = 0$. Below this curve the chemical potential μ remains zero, but $n_c > 0$. *I.e.*, if the initial number density of particles and the energy density correspond to this region, then the condensate forms in the final state. On the contrary, for the region above the solid curve, $\mu < 0$ and $n_c = 0$ in Eq.(2.5). The dashed line on the Fig. 3 corresponds to the variation of the parameter f_0 (keeping the parameter Γ of the initial distribution (3.1) to be fixed, $\Gamma = 5$). With the increase of f_0 the phase point moves along the dashed line from left to right. The choice $f_0 \lesssim f_{\rm crit} \approx 2.8$ corresponds to a Bose-gas density less than critical, while $f_0 > f_{\rm crit}$ corresponds to condensate formation in the final equilibrium state.

B. Kinetics without condensate formation in the equilibrium state

For completeness (and as a particular check of our numerical procedures) let us first consider the case $f_0 \lesssim f_{\rm crit}$. We integrated kinetic equation with two particular values of

f_0, $f_0 = 0.1$ and $f_0 = 1$. In the case $f_0 = 0.1$ the f^3 quantum terms in the function $F(f)$, Eq.(3.3), are small corrections and the kinetic equation reduces to the Boltzmann equation for classical particles, while $f_0 = 1$ is a true quantum regime.

The results of numerical integration of the kinetic equation are presented in Fig. 4. The dashed curve corresponds to the initial distribution function (3.1). The dotted curves represent numerical results at a sequence of moments $\tau \approx 1, 5, 10, 20$. The equilibrium distribution is shown by the solid curve. It is close to the classical Boltzmann distribution in Fig. 4a, and corresponds to the Bose-Einstein distribution (2.5) with $T \approx 0.63\,\varepsilon_0$ and $\mu \approx -0.078\,\varepsilon_0$ in Fig. 4b. We see that already at $\tau \approx 10$ the numerical results are almost indistinguishable from the equilibrium distributions, and by the time $\tau \approx 20$ they coincide identically on the scale of Fig. 4.

On Fig. 5 the value of the distribution function at $\mathbf{p} = 0$ is shown as a function of time for both cases $f_0 = 0.1$ and $f_0 = 1$. We see that the relaxation time is close to 10 in the first case, while $\tau_{\rm rel} \approx 20$ in the second case. However, according to Eq.(3.2) the physical relaxation time in the case $f_0 = 1$ is an order of magnitude shorter, which is the effect of the stimulated scattering.

C. Non-linear quantum kinetic regime or the classical turbulence

Now we turn to the case we are interested in: the Bose-condensate formation. The initial distribution have to correspond to a large values of the parameter f_0, *e. g.* in our case of Eq. (3.1) $f_0 > 2.8$. We shall simplify the problem and consider $f_0 \gg 1$. In this case we can disregard f^2 terms in the function (2.2a), which becomes:

$$F(f) = [f_1 + f_2]f_1' f_2' - [f_1' + f_2']f_1 f_2 \ . \tag{3.5}$$

Parameter f_0 disappears from the kinetic equation and the latter became scale invariant. This scale invariance gives the origin to a self-similar evolution, as we shall see shortly.

As we have noted in the Introduction, very large occupation numbers corresponds to the statistics of classical waves. The kinetic equation with $F(f)$ given by Eq. (3.5) can be obtained directly in a random phase approximation for the classical waves and is well known in the theory of turbulence [17, 21].

We integrated the kinetic equation in the energy interval $10^{-9} < \varepsilon < 10$. We had defined the distribution function on the grid of 200 points equally spaced in the logarithm of energy and used the spline interpolation when calculating the distribution function at intermediate points. We have checked that the grid of 400 points produces essentially identical results. For each integration in collision integral we had implied Gauss algorithm. Particle and energy non-conservation was of order 10^{-3} for the entire time of integration.

The results of the numerical integration of the kinetic equation (2.6) are presented in Fig. 6, where we plot the distribution function at different moments of time. We arranged the output each time that $f(\varepsilon = \varepsilon_{\rm min}, t)$ had increased by one order of magnitude. The most striking feature of this plot is the self-similar character of the evolution. The distribution function has a "core" where $f(\varepsilon) \approx$ const and the radius of the core decreases with time

while the value of $f(\varepsilon)$ in the origin grows. Self-similar solutions exhibiting this kind of behavior can be parametrized as $f(\varepsilon,\tau) = A^{-\beta}(\tau) f_s(\varepsilon/A(\tau))$, where it is assumed $\beta > 0$ and $A(\tau) \to 0$ with the increase of time. Outside the core the distribution function does not depend upon time and is the power law to very good accuracy.

The value of the logarithmic derivative of $f(\varepsilon)$ is plotted in Fig. 6b. The dotted lines in Figs. 6 correspond to the limiting value $\alpha = 7/6$ (see Appendix B 1) but this value is never reached prior to the moment of condensate formation. After that moment the character of the evolution completely changes (see the next Section). Rather, with the boundary condition $df/d\varepsilon = 0$ at $\varepsilon = 0$ the power law on the tail is $\alpha = 1.24$.

We believe that the difference of the exponent in our self-similar distribution from the limiting critical exponent $\alpha = 7/6$ is not a kind of the numerical artifact. In favour of that we have the following arguments:

1. Doubling the number of grid points and/or integrator accuracy does not change the distribution function appreciably. We have tried also different integration algorithms and different boundary conditions at large energies.

2. We had observed that after the particle flux wave reaches the bottom boundary of the integration interval $\varepsilon_{\rm min} = 10^{-9}$ (which happens at $\tau \approx 19$ in our case), the distribution rapidly relaxes to the strict power law $\varepsilon^{-7/6}$ throughout the whole integration interval. This confirms, first, that our integration procedure correctly finds the roots of the equation $I_{\rm coll} = 0$, and, second, that the critical exponent $\alpha = 7/6$ can be achieved with the fitting boundary conditions only, while in our case of condensate formation $f'(0) = 0$. This can explain also why the final distribution observed in Ref. [25] was not resolved from $\alpha = 7/6$. Indeed, the minimum value of the energy on the grid in Ref. [25] was only $\varepsilon_{\rm min} = 10^{-3}$, while we have $\varepsilon_{\rm min} = 10^{-9}$, so the results of Ref. [25] are more effected by the boundary conditions at small ε and this happens in a shorter time.

3. From the analytical point of view the 7/6 critical exponent corresponds to a stationary distribution, *i.e.* to a solution of the equation $I_{\rm coll} = 0$, while the shape of the self-similar distribution is defined by Eq. (5.3b) below, with yet to be determined parameter β which does not have to coincide with 7/6.

The time dependence of the distribution function at $\varepsilon = 0$ is shown in Fig. 7 by the solid line. Vertical dot-dashed line corresponds to $\tau = \tau_c$ and the distribution function asymptotically tend to this line according to the law $f(0,\tau) \propto (\tau_c - \tau)^{-2.6}$, which is shown by the dotted line on this figure. It is possible to find this time dependence at $\varepsilon = 0$ analytically, using the self-similarity of the solution, see Section V.

D. Condensation in the presence of condensate

In the previous subsection we have seen that the distribution function of particles prior to the condensate formation tend to the power law with the exponent α been almost constant, see Fig. 6. As one set of initial conditions for the condensation in the presence of the condensate we took the final distribution shown in Fig. 6. Though the limiting value of 7/6 was not reached prior to condensate formation, this exponent is the special one and represents the root of the equation $I_{\rm P} = 0$, see Appendix B. Because of that we have chosen

the function

$$f(\varepsilon) = C\,\varepsilon^{-7/6} e^{-\varepsilon} \tag{3.6}$$

for the second set of the initial conditions while integrating Eqs.(2.9). In Eq. (3.6) C is some normalization constant, $C = 1$ corresponds roughly to the magnitude of the final distribution at $\varepsilon \sim \varepsilon_{\rm min}$ presented in Fig. 6a. We took initially $n_c \ll n_{\rm tot}$. We will see shortly that the particular choice for n_c, as far as this condition is satisfied, is insignificant.

First let us discuss the case with the initial condition (3.6). The results of the numerical integration of the system (2.9) are presented in Fig. 8. The dashed line corresponds to the initial distribution. Solid lines correspond to the distribution function $f(\varepsilon)$ at different moments of time. Basically, evolution proceeds in the following way. First, the power law $f(\varepsilon) \propto \varepsilon^{-7/6}$ changes to the law $f(\varepsilon) \propto 1/\varepsilon$ at small energies. And then this change propagates to the region of larger energies, see Figs. 9,10. Later on the power law stays at the equilibrium value $\alpha = 1$, but the amplitude of the distribution function gradually decreases. The same kind of behavior of $f(\varepsilon, t)$ was found also in the paper [25].

Again, we see that the essential part of the curves in Fig. 8b repeats itself under translation from left to right and the evolution is self-similar. During this epoch (before "the wave of change" had reached the exponential tail of the initial distribution at $\varepsilon > 1$) approximately 40% of particles had condensed. And, what is important, the number of particles in the condensate grows linearly with time at this epoch, $n_c/n_{\rm tot} = B\tau$. We found $B \approx 2\,C^2$. This enables us to eliminate the ambiguity in the initial value for n_c since B does not depend upon it. Indeed, in our simulations which were done in a finite energy interval, during the first several iterations the system self-adjusts: A proper profile of the distribution forms while the condensate reaches a particular value of n_c. We can disregard this period and extrapolate the curves in Fig. 8b, $n_c(\tau)$, and the self-similar character of the evolution back in time and to the region of smaller energies.

The fraction of particles in condensate as a function of time is presented in Fig. 9.

With the final distribution in Fig. 6 taken as the initial condition for the condensation in the presence of the condensate the fraction of condensed particles increases with time dramatically differently initially. Instead of $n_c/n_{\rm tot} \propto \tau$ we obtain now $n_c/n_{\rm tot} \propto \sqrt{\tau}$. Both exponents can be understood analyzing self-similar solutions, see Section V B.

IV. INTERACTION WITH ZERO TEMPERATURE FERMION BATH

In this Section we consider ideal bose gas coupled to a fermion heat bath of infinite capacity. The function F in the kinetic equation (2.6) in this case is defined by Eq. (2.2b) and $|M_{fi}|^2 = g^4$.

For simplicity and definiteness we shall consider fermions at zero temperature, $T_{\rm bath} = 0$. The corresponding distribution function of fermions has the form $\eta(\varepsilon) = \theta(\mu - \varepsilon)$, where μ is the Fermi energy. Such a simple form of the fermion distribution function allows us to make one more analytical integration in the collision integral; at the end only one integration remains to be calculated numerically. The price being paid for that is the increased complexity of the final analytical expression which we put therefore in Appendix C.

As an initial distribution we choose the function which has an equilibrium form:

$$f_{\rm in}(\varepsilon) = \frac{1}{\exp\left[(\varepsilon - \mu_{in})/T_{\rm in}\right] - 1} \ , \tag{4.1}$$

where $T_{\rm in}$ and $\mu_{\rm in}$ are initial temperature and chemical potential of the Bose system correspondingly. In what follows we choose the energy scale ε_0 and define the particle energy, the chemical potential and the temperature in units of ε_0. To this end we choose $f_{\rm in}(\varepsilon = 1) = 1$, which gives us the relation $\mu_{\rm in} = [1 - \log(2)]T_{\rm in}$. Under this condition only one dimensionless parameter $T_{\rm in}$ is left to define the initial state of Bose particles.

The parameter ε_0 after rescaling will not enter the kinetic equation explicitly, but will define the time scale of the evolution. We define the dimensionless time τ as

$$\tau = \frac{\varepsilon_0^2 g^4}{64\pi^3 m} \ t \ . \tag{4.2}$$

We had specified the initial distribution Eq. (4.1) choosing $T_{\rm in} = 2$. For the Fermi energy we have used $\mu_F = 20$. Since $T_{\rm bath} = 0$, all Bose particles has to condense eventually.

We integrated kinetic equation in the energy interval $10^{-8} < \varepsilon < 100$. We defined the distribution function on the grid of 661 points equally spaced in the logarithm of energy and used Spline interpolation when calculating distribution function at intermediate points. We had implied Simpson algorithm on the grid of the same size for the collision integral . The non-conservation of particle number over the integration time $\tau \approx 20$ was $\delta n/n = 0.001\%$.

The results of numerical integration of the kinetic equation (C1) are presented on Fig. 10, where we plot the distribution function at several different moments of time. The distribution function behaves completely differently now as compared to the case of self-interacting bosons. It narrows in time gradually approaching a δ- function [13].

The value of the distribution function at zero energy (see Fig. 11) tend to infinity with time only as τ^3. Consequently, it would require infinite time for the distribution function to reach the infinity. This does not necessarily means that the condensation time is infinite in this case (see the corresponding discussion in the Introduction), but means that in this simple approach we can not find the condensation time-scale for the ideal Bose gas coupled to the thermal bath. However, we still can find the upper limit on the condensation time-scale, even without the knowledge when the phase transition to the condensed phase takes place actually. Indeed, the interaction with fermions necessarily leads to the self-interaction in higher orders of the perturbation theory (consider the box diagram constructed from the diagram Fig. 1b) with $\lambda \sim g^4$. When the product $g^4 f(0)$ exceeds O(1), this induced self-interaction starts to dominate, and the problem reduces to the previous case of self-interacting bosons with the explosive grows of the distribution function.

V. SELF-SIMILARITY AND ANALYTICAL SOLUTIONS

The results of the numerical integration presented in previous sections suggest that during condensate formation the distribution function evolve in a self-similar way. Assuming self-similarity from the very beginning we can simplify the kinetic equation and then a number

of analytical results can be obtained [25, 22, 23]. In this section we discuss this analytical approach and compare it to the numerical results.

We parametrize self-similar solutions as

$$f(\varepsilon,\tau) = A^{-\beta}(\tau) f_s(\tilde{\varepsilon}) \ , \tag{5.1}$$

where $\tilde{\varepsilon} \equiv \varepsilon/A(\tau)$ and β is some constant. For definiteness we shall assume $\beta > 0$, *i.e.* in the following subsections **A** and **C**, where we shall consider the epoch prior to the condensate formation (when $f(0,\tau)$ has to grow), $A(\tau) \to 0$ as time τ increases , while $A(\tau)$ will be growing function of time in subsection **B** which describes the epoch after the condensate has formed. We always can choose the normalization $f_s(0) = 1$ if $f_s(0)$ is finite, which is the case in subsections **A** and **C**, and $A(0) = 1$ otherwise.

Self-similar solutions appear when the phase-space density is large, $f + 1 \approx f$, in which case the kinetic equation became invariant with respect to the rescaling. This condition is satisfied around the condensate formation, and as we have seen, the system approaches self-similar solutions starting with arbitrary initial conditions. We assume $f(\varepsilon) \gg 1$ everywhere below.

A. Self-interacting bosons prior to condensate formation

Substituting parametrization (5.1) into kinetic equation (2.6) we obtain:

$$-A^{-\beta-1}\dot{A}\ [\beta f_s(\tilde{\varepsilon}) + \tilde{\varepsilon}\frac{df_s(\tilde{\varepsilon})}{d\tilde{\varepsilon}}] = \frac{I_{\rm P}[f_s(\tilde{\varepsilon})]}{A^{3\beta-2}} \ . \tag{5.2}$$

Separating variables we find

$$-A^{2\beta-3}\dot{A} = C_s \ , \tag{5.3a}$$

$$\beta f_s(\tilde{\varepsilon}) + \tilde{\varepsilon}\frac{df_s(\tilde{\varepsilon})}{d\tilde{\varepsilon}} = \frac{I_{\rm P}[f_s(\tilde{\varepsilon})]}{C_s} \ , \tag{5.3b}$$

where C_s is (positive) separation constant. Integrating the first equation in (5.3) we obtain:

$$A(\tau) = [2C_s(\tau_c - \tau)(\beta - 1)]^{1/2(\beta-1)} \ , \tag{5.4}$$

where τ_c is the integration constant apparently corresponding to the moment of time of the condensate formation. Indeed, the distribution function at zero momentum as a function of time is $f(0,\tau) = A(\tau)^{-\beta}$, and $f(0,\tau)$ has the pole at $\tau = \tau_c$ if $\beta > 1$.

We can conclude from Fig. 6a that at the tail where the distribution function is a power law, $f \propto \varepsilon^{-\alpha}$, it does not depend upon time. According to Eq. (5.1) this means that $\beta = \alpha$. This concludes the derivation of the function $f(0,\tau)$ for the self-similar solution, which is plotted in Figs. 7(a,b) by the dotted line using $\alpha = 1.24$. This value of α can be extracted from Fig. 6b . The agreement of this function with direct numerical result is very good, see Fig. 7b. We conclude, that after the solution have reached self-similar form, the time dependence of the distribution function at zero momentum is given by

$$f(0,\tau) \propto (\tau_c - \tau)^{-\alpha/2(\alpha-1)} \propto (\tau_c - \tau)^{-2.6} \ , \tag{5.5}$$

which reaches infinity at a finite time. Note that with the critical value $\alpha = 7/6$ we would obtain $f(0,\tau) \propto (\tau_c - \tau)^{-3.5}$. This function is plotted by the dashed line in Fig. 7b and is quite different from what we observe numerically.

B. Self-interacting bosons and the condensate

Substituting parametrization Eq. (5.1) into Eqs. (2.9) we obtain:

$$\frac{dn_c(\tau)}{d\tau} = n_c(\tau) A(\tau)^{2-2\beta} I_c \ , \tag{5.6a}$$

$$\dot{A}(\tau) A(\tau)^{-\beta-1} \left[\beta f_s(\tilde{\varepsilon}_1) + \tilde{\varepsilon}_1 \frac{df_s(\tilde{\varepsilon}_1)}{d\tilde{\varepsilon}_1} \right] = -A(\tau)^{2-3\beta} I_P(\tilde{\varepsilon}_1) - n_c(\tau) A(\tau)^{(1-4\beta)/2} I_{pc}(\tilde{\varepsilon}_1) \ , \tag{5.6b}$$

where I_c and I_{pc} are integrals in r.g.s. of Eqs. (2.9a) and (2.9b) respectively. Under the condition

$$n_c(\tau) = C_n A(\tau)^{(3-2\beta)/2} \ . \tag{5.7}$$

variables in Eq. (5.6b) separates:

$$\dot{A}(\tau) A(\tau)^{-\beta-1} = A(\tau)^{2-3\beta} C_s \ , \tag{5.8a}$$

$$-C_s \left[\beta f_s(\tilde{\varepsilon}_1) + \tilde{\varepsilon}_1 \frac{df_s(\tilde{\varepsilon}_1)}{d\tilde{\varepsilon}_1} \right] = I_P(\tilde{\varepsilon}_1) + C_n I_{pc}(\tilde{\varepsilon}_1) \ . \tag{5.8b}$$

If we solve Eq. (5.7) with respect to $A(\tau)$ and substitute it into Eq.(5.6a) we find

$$n_c(\tau) = C_n \left[\frac{4(1-\beta) I_c}{(2\beta - 3)} \tau \right]^{(3-2\beta)/4(\beta-1)} \ , \tag{5.9}$$

which gives the time dependence of the number of condensed particles. As a self-consistency check we find that the same substitution, but with Eq. (5.7) solved with respect to $n_c(\tau)$, gives the condition equivalent to Eq. (5.8a) if $C_s = 2I_c/(3-2\beta)$. This defines C_s. The solution of Eq.(5.8a) is:

$$A(\tau) = \left[1 + \frac{4(1-\beta) I_c}{(2\beta - 3)} \tau \right]^{1/2(\beta-1)} \ . \tag{5.10}$$

As we have seen, the equilibrium profile $f \propto 1/\varepsilon$ propagates from the region of small energies to the region of large energies as a "wave", leaving $f \propto \varepsilon^{-\alpha}$ to be time independent

in the region which this "wave" has not reached yet. This, again, means that $\beta = \alpha$. With $\alpha = 7/6$ as an initial condition we find from Eq. (5.9) that the condensate linearly grows with time, $n_c(\tau) = \text{const} \times \tau$. This is in agreement with the results of our numerical experiment, see Fig. 9. This self-similar regime persisted till the "wave" have reached exponential tail where α is different. During this period $\approx 40\%$ of particles had condensed. With the initial condition $\alpha = 1.24$ we obtain dramatically different rate of condensate growth, $n_c(\tau) \propto \tau^{0.54}$ which, again, was confirmed by the direct numerical integration.

C. Interaction with degenerate Fermi gas

Now we substitute parametrization (5.1) into the kinetic equation with the function F given by Eq. (2.2b). Left-hand side of equation (5.2) remains unchanged in this case, however, its right-hand side reads now $I[f_s(\tilde{\varepsilon})]/A^{2\beta-2}$. This changes equation (5.3a) to

$$\dot{A} = -A^{3-\beta}\, C_s \ . \tag{5.11}$$

In the case of the self-interacting bosons we were able to find β using the information gained from the numerical integration that on the tail of the self-similar distribution the value of f does not depend upon time. That gave us $\beta = \alpha$ and we have extracted α as a logarithmic derivative of the distribution function with respect to the energy. We could not use integrals of the motion in that case since the particle number (as well as the energy density) saturated at the very end of the distribution where the self-similarity does not hold anymore (since on the self-similar solution we had $\alpha < 3/2$). Now, on the contrary, the particle number saturates already near the core of the self-similar distribution, see Fig. 10 (moreover, α grows with time). This enables us to find β using conservation of particles.

Substituting parametrization (5.1) into Eq. (3.4b) we find $\beta = 3/2$. Consequently, the equation (5.11) reads now $\dot{A} = -A^{3/2}\, C_s$. We find finally that

$$f(\varepsilon = 0, \tau) = A^{-3/2} \propto (\tau + \tau_0)^3 \ . \tag{5.12}$$

This is in good agreement with the results of our numerical integration, see Fig. 11.

The ε-dependence of the distribution function can be found from the equation (5.3b), which in the limit of large μ takes the form

$$\frac{3f_s}{2} + \tilde{\varepsilon}\frac{df_s}{d\tilde{\varepsilon}} = \frac{f_s}{C_s}\left[\frac{1}{\sqrt{\tilde{\varepsilon}}}\int_0^{\tilde{\varepsilon}} dx x^{1/2}(x-\tilde{\varepsilon})f_s(x) + \int_{\tilde{\varepsilon}}^{\infty} dx(x-\tilde{\varepsilon})f_s(x)\right] \tag{5.13}$$

Let us make here the connection to results of Ref. [13]. One can see that it is possible to rewrite the final expressions of [13] in a self-similar form, Eq. (5.1), with the same value of $\beta = 3/2$ and the same function $A(\tau) \propto \tau^{-2}$ at large τ. This gives $f_s = f_s(\sqrt{\varepsilon}\tau)$. Using this and noting that Levich and Yakhot started from the initial conditions corresponding to the critical point, $f_s(\tilde{\varepsilon}) \propto 1/\tilde{\varepsilon}$, we find their result $f(\varepsilon, \tau) \propto \tau$. Our direct numerical integrations with an appropriate initial conditions confirm that. However, in the runs the results of which we had reported above we have had different boundary conditions, $f_s(0) = 1$, which leads

to $f(0,\tau) \propto \tau^3$ at large τ, Eq. (5.12). We see that the system which is father away from the critical point condenses with a higher rate.

The solution found in Ref. [13] for f_s, which with our initial and boundary conditions corresponds to $f_s(\tilde{\varepsilon}) = \exp(-\sigma\sqrt{\tilde{\varepsilon}})$, is not an exact solution to equation (5.13), however, it is a reasonable approximation. This solution is plotted in Fig. 10 by the dotted line.

VI. CONCLUSIONS AND DISCUSSION

We have studied numerically the kinetics of condensation of the weakly interacting Bose gas. We have found that the distribution function evolves very differently in cases of Bose-bath interaction and self-interaction of Bose particles. This results from the different structure of the kinetic equations describing particle-bath and particle-particle interactions [the latter contains extra powers of $f(\varepsilon)$]. In the first case the distribution function of the excess particles, which eventually form the condensate, narrows gradually with time and continuously approaches a δ- function in infinite time, as it was found in Ref. [13] assuming small energy exchange per collision.

For the case of self-interacting bosons we find, in qualitative agreement with Refs. [25, 16], that the singular power law profile $f(\varepsilon) \propto \varepsilon^{-1.24}$ of the distribution function forms in a finite time. This is close to $f(\varepsilon) \propto \varepsilon^{-7/6}$ which is a stationary solution of the kinetic equation and corresponds to the constant flux of particles in momentum space towards the condensate. Different exponents result from different boundary conditions during the Bose condensation, namely $\partial f/\partial\varepsilon(0,t) = 0$, as opposed to the case of stationary turbulence. While the exponents differ by only 6% this leads to significantly different values for other critical exponents, *e.g.* β in $f(0,t) \propto (t_c - t)^{-\beta}$, or for the rate of the condensate growth γ in $n_c \propto t^{\gamma}$. We have found $\beta = 2.6$ and $\gamma = 0.54$, while for $f(\varepsilon) \propto \varepsilon^{-7/6}$ we would have $\beta = 3.5$ and $\gamma = 1$.

One could expect that this very natural regime of the constant flow of particles into the condensate will persist in the presence of the condensate as well until all excess particles from the high energy tail are in the ground state. Nevertheless, this is not the case and at the moment the condensate appears, its presence terminates this regime. Instead of such a steady flow through the entire energy interval, particles from all energy levels jump directly to the condensate, while the remaining particles maintain an equilibrium shape of the distribution function $f(\varepsilon) \propto \varepsilon^{-1}$. The constant of proportionality in this law gradually decreases until it reaches an equilibrium value.

The build up of coherence cannot be observed in the framework of the Boltzmann kinetic equation, but the kinetic description has to be valid prior to and after the moment of condensate formation. We have seen that evolution at both stages is self-similar. This allows us to obtain a number of useful analytical relations, *e.g.* the time dependence of the distribution function near the point of condensate formation, Eq. (5.4), and Eq. (5.9) for the subsequent growth of the condensate. We have found the duration of both stages, which is finite and of order $\tau_c \sim 20$.

Our results of numerical integration of the Boltzmann equation might be used as an initial condition in a theory of condensate nucleation.

Another interesting application of our results could be in a description of Bose-star formation. A complete theory of this process requires the inclusion of gravity and the problem is more involved. While the isotropy in momentum space will be broken, the kinetics of Bose relaxation in the collapsing core can proceed largely along the lines described in the present paper. Moreover, the relaxation time can become shorter, since the spatial collapse of the core under the influence of self-gravity would cause an additional increase of the density of particles, which would speed up the relaxation.

It is remarkable that in spite of the apparent smallness of the axion quartic self-coupling, $\lambda_a^4 \sim 10^{-53} f_{12}^{-4}$ (where $f_{12} = f_a/10^{12}$ GeV) the relaxation time in axion miniclusters can be comparable to the age of the universe [7, 8]. This is because the relevant quantity is not the self-coupling itself, but the product of λ with the mean field strength squared (or with the mean phase-space density of "particles", which in the present case would rather be the phase-space density of classical scalar waves). For particles bound in a gravitational well, it is convenient to rewrite the expression for the relaxation time in the form $\tau_c \sim m^7 \lambda^{-2} \rho^{-2} v_e^2$ [7], where ρ is the energy density in a minicluster and v_e is the escape velocity. For axions, the relaxation time is smaller than the present age of the Universe if the energy density satisfies $\rho_{10} > 10^6 v_{-8} \sqrt{f_{12}}$, where $\rho_{10} \equiv \rho/(10\,\mathrm{eV})^4$ and $v_{-8} \equiv v_e/10^{-8}$. It was shown in Refs. [8] that those large densities can be achieved naturally in axion miniclusters and, therefore, a "Bose-star" can form [26].

Our results are applicable whenever Eq. (2.1) holds and might also be interesting for a study of, *e.g.*, Kolmogorov turbulence.

ACKNOWLEDGMENTS

We thank V. A. Berezin, E. W. Kolb, V. A. Rubakov, G. Starkman and F. V. Tkachov for useful discussions. This work was supported by DOE and NASA grant NAG5-2788 at Fermilab. D.S. thanks the Astrophysics Department of FNAL for the hospitality during this work.

APPENDIX A: REDUCTION OF THE COLLISION INTEGRAL

In this Appendix we will make as many integrations in the collision integral analytically, as it is possible. In the case we are interested in, *i.e.*, four-particle interaction vertex and the isotropic one-particle distribution function, seven out of nine integrations can be done and only two integrals upon the energies of incoming particles remain the for numerical treatment. We start from the non-relativistic counterpart of Eq.(2.1)

$$I_{\mathrm{coll}} = \frac{(2\pi)^4}{16m^4} \int \delta^4(\sum_i p_{\mu i}) |M_{fi}(|\mathbf{p}|)|^2 F(f) \prod_i \frac{d^3\mathbf{p}_i}{(2\pi)^3} \ , \tag{A1}$$

where $F(f)$ is defined in (2.2) with the distribution function f which depends upon particle energy ε only. We shall make use of the identity

$$\delta^3(\sum \mathbf{p}_i) = \int e^{i(\lambda,\mathbf{p}_1+\mathbf{p}_2-\mathbf{p}_1'-\mathbf{p}_2')} \frac{d^3\lambda}{(2\pi)^3} \tag{A2}$$

and explicitly separate out angle integrations

$$d^3p_i = d\phi_i d\cos\theta_i p_i^2 dp_i \equiv m p_i d\Omega_i d\varepsilon_i \ . \tag{A3}$$

Collision integral (A1) takes the form:

$$I_{\rm coll} = \frac{|M_{fi}|^2}{64\pi^3 m} \int \delta(\varepsilon_1+\varepsilon_2-\varepsilon_1'-\varepsilon_2') F(f) D d\varepsilon_1' d\varepsilon_2' d\varepsilon_2 \ . \tag{A4}$$

where we have assumed that the matrix element does not depend upon momenta and we have defined

$$D \equiv \frac{p_2 p_1' p_2'}{64\pi^5} \int \lambda^2 d\lambda \int e^{i(\mathbf{p}_1,\lambda)} d\Omega_\lambda \int e^{i(\mathbf{p}_2,\lambda)} d\Omega_{p_2} \int e^{i(\mathbf{p}_1',\lambda)} d\Omega_{p_1'} \int e^{i(\mathbf{p}_2',\lambda)} d\Omega_{p_2'} \ . \tag{A5}$$

All angle integrals are trivial in (A5) and we get

$$D = \frac{4}{\pi p_1} \int_0^\infty \frac{d\lambda}{\lambda^2} \sin(\lambda p_1)\sin(\lambda p_2)\sin(\lambda p_1')\sin(\lambda p_2') \ . \tag{A6}$$

After some algebra and taking into account the energy conservation condition this gives

$$D = \frac{1}{p_1} \min[p_1, p_2, p_1', p_2'] \ . \tag{A7}$$

Now, the energy δ-function can be trivially integrated away and we are left with two-dimensional integral upon energies of incoming particles [19]

$$\frac{df(\varepsilon_1)}{dt} = \frac{|M_{fi}|^2}{64\pi^3 m} \int\int F(f) D d\varepsilon_1' d\varepsilon_2' \ , \tag{A8}$$

where $\varepsilon_2 = \varepsilon_1' - \varepsilon_2' - \varepsilon_1$.

APPENDIX B: STATIONARY SOLUTIONS TO THE KINETIC EQUATION

1. Kolmogorov's spectra

In this Appendix we shall describe power law solutions of the equation $I_{\rm coll} = 0$. We shall consider the region of large values of the distribution function, $f(\varepsilon) \gg 1$, *i.e.*, $F(f)$ will be given by Eq. (3.5). The kinetic equation with this form of $F(f)$ was extensively studied in the literature devoted to the problem of the Kolmogorov turbulence [18], and in Ref. [19] all power law solutions to the equation $I_{\rm coll} = 0$ were found. Two of those solutions are evident. One is just the limit of the Eq.(2.5) at $\varepsilon \to 0$, and $n_c = 0$ and has the form $f = {\rm const}/\varepsilon$. Another one is $f = {\rm const}$. Both are solutions to a simpler equation $F(f)\delta(\sum \varepsilon) = 0$. To find the remaining solutions is a non-trivial task and with the distribution function of the form $f(\varepsilon) = \varepsilon^{-\alpha}$ the trick is to map all labelled regions in Fig. 2 to the region I by means of Zakharov transformations [19]:

II $\to$ I	III $\to$ I	IV $\to$ I
$\varepsilon_1' \to \varepsilon_1\varepsilon_2'/\varepsilon_2$	$\varepsilon_1' \to \varepsilon_2\varepsilon_1/\varepsilon_2'$	$\varepsilon_1' \to \varepsilon_1^2/\varepsilon_1'$
$\varepsilon_2' \to \varepsilon_1\varepsilon_1'/\varepsilon_2$	$\varepsilon_2' \to \varepsilon_1^2/\varepsilon_2'$	$\varepsilon_2' \to \varepsilon_2\varepsilon_1/\varepsilon_1'$

where $\varepsilon_2 = \varepsilon_1' + \varepsilon_2' - \varepsilon_1$. Under this transformations the sum of integrals over regions I - IV can be represented as an integral over the region I only:

$$\int\int_{(\mathrm{I})} (\varepsilon_1'\varepsilon_2'\varepsilon_2)^\alpha \left[1 + \left(\frac{\varepsilon_2}{\varepsilon_1}\right)^\alpha - \left(\frac{\varepsilon_1'}{\varepsilon_1}\right)^\alpha - \left(\frac{\varepsilon_2'}{\varepsilon_1}\right)^\alpha\right] \left[1 + \left(\frac{\varepsilon_2}{\varepsilon_1}\right)^\beta - \left(\frac{\varepsilon_1'}{\varepsilon_1}\right)^\beta - \left(\frac{\varepsilon_2'}{\varepsilon_1}\right)^\beta\right] d\varepsilon_1' d\varepsilon_2' \,, \tag{B1}$$

where $\varepsilon_2 = \varepsilon_1' + \varepsilon_2' - \varepsilon_1$ and $\beta = -7/2 + 3\alpha$. We see that in fact there are four solutions to the equation $I_{\mathrm{coll}} = 0$ which correspond to $\alpha = 0$, 1 or $\beta = 0$, 1. This gives

$$\alpha = 0, \quad \alpha = 1, \quad \alpha = 7/6, \quad \alpha = 3/2 \quad . \tag{B2}$$

Our numerical self-similar solution, Fig. 6, tend to the power law $f = \varepsilon^{-7/6}$; however, it never reaches this critical exponent prior to the condensate formation, see Figs. 7 and 8. Physically the solution with $\alpha = 7/6$ corresponds to the constant flux of the particle number from the region of lager energies towards the future condensate.

2. Solutions in the presence of condensate

In the presence of the condensate the number and the nature of zeros of the collision integral changes. The kinetic equation can be represented as a system of two equations, Eqs.(2.9). The collision integral in Eq.(2.9b) consists of two terms. The first term, I_{p}, is the same as in the absence of the condensate, and the corresponding integral is zero on the solutions corresponding to the same values of α, Eq.(B2). However, the second term does not. Assuming the power law $f(\varepsilon) = \varepsilon^{-\alpha}$, the integration in this term can be made analytically with the result proportional to

$$\varepsilon^{1-2\alpha} \left[\frac{4}{\alpha - 1} + \frac{4^\alpha \Gamma(1-\alpha)(\pi + \Gamma(\frac{3}{2} - \alpha)\Gamma(\alpha - \frac{1}{2}))}{2\sqrt{\pi}\Gamma(\frac{3}{2} - \alpha)}\right] . \tag{B3}$$

This expression as a function of α has two zeros only at

$$\alpha = 1 \quad \text{and} \quad \alpha = 3/2 \quad , \tag{B4}$$

and consequently the total collision integral in Eq.(2.9b) is zero on those exponents only. Moreover, the collision integral in Eq.(2.9a) is zero with $\alpha = 1$ only. This explains why the power law $f(\varepsilon) = \varepsilon^{-7/6}$ changes to $f(\varepsilon) = \varepsilon^{-1}$ in the presence of the condensate, see Fig. 8b.

APPENDIX C: KINETIC EQUATION FOR IDEAL BOSONS INTERACTING WITH DEGENERATE FERMI GAS

Assuming fermions to be at zero temperature, *i.e.*, their distribution function to be given by $\eta(\varepsilon) = \theta(\mu - \varepsilon)$, allows us to make one more integration in Eq. (2.6) analytically. After some algebra we obtain:

$$\frac{df(\varepsilon)}{d\tau} = f(\varepsilon)(J_1 + J_2) + [f(\varepsilon) + 1](J_3 + J_4)\,, \tag{C1}$$

where

$$J_1 = -\frac{\eta(\varepsilon)}{\sqrt{\varepsilon}} \int_0^\varepsilon dx x^{1/2}(\varepsilon - x)[f(x) + 1]\ , \tag{C2a}$$

$$J_2 = \frac{2(1-\eta(\varepsilon))}{3\sqrt{\varepsilon}} \left\{ \int_0^\mu dx x^{3/2}[f(x+\varepsilon-\mu)+1] - \mu^{3/2} \int_\mu^\varepsilon dx[f(x)+1] \right. \\ \left. - \int_0^\mu dx x^{1/2}(\mu - \frac{x}{3})[f(x)+1] \right\} \tag{C2b}$$

$$J_3 = \eta(\varepsilon) \left\{ \int_\varepsilon^\mu dx(x-\varepsilon)f(x) + \int_\mu^\infty dx(\mu - \frac{\varepsilon}{3})f(x) - \frac{2}{3\sqrt{\varepsilon}} \int_0^\varepsilon dx x^{3/2} f(\mu + \varepsilon - x) \right\} \tag{C2c}$$

$$J_4 = \frac{2(1-\eta(\varepsilon))}{3\sqrt{\varepsilon}} \left\{ \int_\varepsilon^\infty dx \mu^{3/2} f(x) - \int_0^\mu dx x^{3/2} f(\mu + \varepsilon - x) \right\} \tag{C2d}$$

where μ is the Fermi energy. This equation was subject to the numerical integration in Section IV.

REFERENCES

[1] E.M.Lifshitz and L.P.Pitaevskii, *Statistical Physics*, Nauka, Moscow, 1978 (Pergamon, Oxford, 1980)

[2] For reviews see: T. J. Greytak and D. Kleppner, in *New Trends in Atomic Physics*, ed. by G. Grynberg and R. Stora (North-Holland, Amsterdam, 1984), Vol. 2, 1125; I. F. Silveria and J. T. M. Walraven, in *Progress in Low Temperature Physics*, ed. by D. F. Brewer (North-Holland, Amsterdam, 1986), Vol. 10, p. 139.

[3] H. F. Hess, *et. al.* Phys. Rev. Lett. **59**, 672 (1987); R. van Roijen, *et. al.* Phys. Rev. Lett. **61**, 931 (1988); N. Masuhara, *et. al.* Phys. Rev. Lett. **61**, 935 (1988); J. M. Doyle, *et. al.* Phys. Rev. Lett. **67**, 603 (1991).

[4] C. Monroe, *et. al.* Phys. Rev. Lett. **65**, 1571 (1990); C. R. Monroe, *et. al.* Phys. Rev. Lett. **70**, 414 (1993); A. J. Moerdijk, *et. al.* Phys. Rev. Lett. **72**, 40 (1994); A. J. Moerdijk and B. J. Verhaar, Phys. Rev. Lett. **73**, 518 (1994).

[5] E. Hanamura and H. Haug, Phys. Rep. **C33**, 210 (1977); D. Snoke, J. P. Wolfe, and A. Mysyrowicz, Phys. Rev. Lett. **59**, 827 (1987).

[6] R. Ruffini and S. Bonozzola, Phys. Rev. **187**, 1767 (1969); J. D. Breit, S. Gupta and A. Zaks, Phys. Lett. **140B**, 329 (1984); M. Colpi, S. L. Shapiro and I. Wasserman, Phys. Rev. Lett. **57**, 2485 (1986); I. I. Tkachev, Sov. Astron. Lett. **12**, 305 (1986); J. J. van Der Bij and M. Gleiser, Phys. Lett. **194B**, 482 (1987); R. Friedberg, T. D. Lee and Y. Pang, Phys. Rev. **D35**, 3640 (1987); M. Gleiser, Phys. Rev. **D38**, 276 (1988); E. Seidel and Wai-Mo Suen, Phys. Rev. **D42**, 384 (1990); A. R. Liddle and M. S. Madsen, Int. J. Mod. Phys. **D1**, 101 (1992).

[7] I. I. Tkachev, Phys. Lett. **B261**, 289 (1991).

[8] E. W. Kolb and I. I. Tkachev, Phys. Rev. Lett. **71**, 3051 (1993); Phys. Rev. **D49**, 5040 (1994); *ibid* **D50**, 769 (1994).

[9] For recent reviews, see: M. S. Turner, *Phys. Rep.* **C197**, 67 (1990); G. G. Raffelt, *Phys. Rep.* **C198**, 1 (1990).

[10] D. V. Semikoz and I. I. Tkachev, Phys. Rev. Lett. **74**, 3093 (1995).

[11] H. T. C. Stoof, Phys. Rev. Lett. **66**, 3148 (1991); Phys. Rev. **A45**, 8398 (1992).

[12] M. Inoue and E. Hanamura, J. Phys. Soc. Jpn **41**, 771 (1976).

[13] E. Levich and V. Yakhot, Phys. Rev. **B15**, 243 (1977); see also S. G. Tikhodeev Zh. Eksp. Teor. Fiz. **97**, 681 (1990) [Sov. Phys. JETP **70** 380 (1990)]

[14] E. Levich and V. Yakhot, J. Phys. **A11**, 2237 (1978).

[15] D. W. Snoke and J. P. Wolfe, Phys. Rev. **B39**, 4030 (1989).

[16] Yu. M. Kagan, B. V. Svistunov and G. V. Shlyapnikov, Zh. Eksp. Teor. Fiz. **101**, 528 (1992) [Sov. Phys. JETP **74**, 279 (1992)]; *Errata, ibid* **75**, 387 (1992).

[17] A. S. Monin and A. M. Yaglom, *Statistical Fluid Mechanics: Mechanics of Turbulence* (The MIT press, Vol 1 1971, Vol 2 1975).

[18] A. N. Kolmogorov, Dokl. Akad. Nauk SSSR **30**, 299 (1941).

[19] V. E. Zakharov, Zh. Eksp. Teor. Fiz. **51**, 688 (1967) [Sov. Phys. JETP **24**, 455 (1967)]; *ibid* Zh. Eksp. Teor. Fiz. **62**, 1745 (1972) [Sov. Phys. JETP **35**, 908 (1972)].

[20] V. E. Zakharov and E. A. Kuznetsov, Zh. Eksp. Teor. Fiz. **75**, 904 (1978) [Sov. Phys. JETP **48**, 458 (1978)].

[21] For reviews see: V. E. Zakharov, S. L. Musher and A. M. Rubenchik, Phys. Rep. **C129**, 285 (1985); V. E. Zakharov, *Kolmogorov spectra in weak turbulence problems*, in : Basic Plasma Physics II, ed A. A. Galeev and R. N. Sudan (North-Holland, Amsterdam, 1984).

[22] G. E. Falkovich and A. V. Shafarenko, J. Nonlinear Sci. **1**, 457 (1991).

[23] V. E. Zakharov, V. S. L'vov, G. Falkovich, *Kolmogorov Spectra of Turbulence* (Springer-Verlag, 1992).

[24] U. Eckern, J. of Low Temp. Phys. **54**, 333 (1984); T.R. Kirkpatric and J. R. Dorfman, J. of Low Temp. Phys. **58**, 301 (1984); Phys. Rev. **A28**, 2576 (1983)

[25] B. V. Svistunov, J. Moscow Phys. Soc. **1**, 373 (1991).

[26] Note in this respect that there is another mechanism leading to axion Bose-star formation in miniclusters, namely the "gravitational cooling", which can dominate in some cases, see E. Seidel and W.-M. Suen, Phys. Rev. Lett. **72**, 2516 (1994).

FIGURES

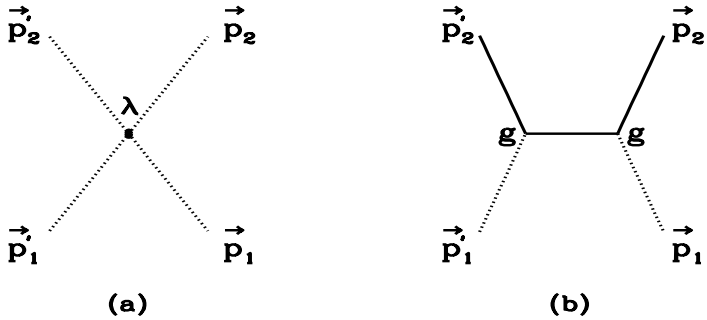

FIG. 1. The scattering processes we consider in Eq. (2.1). (a) is the case of self-interacting bosons, and (b) is the case of ideal Bose gas interacting with the cold fermion bath.

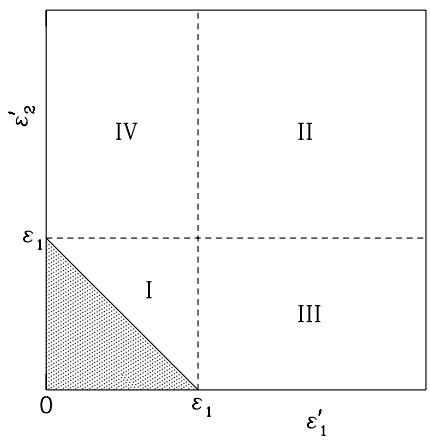

FIG. 2. The white areas correspond to the integration region in the collision integral, Eq. (2.6)

.

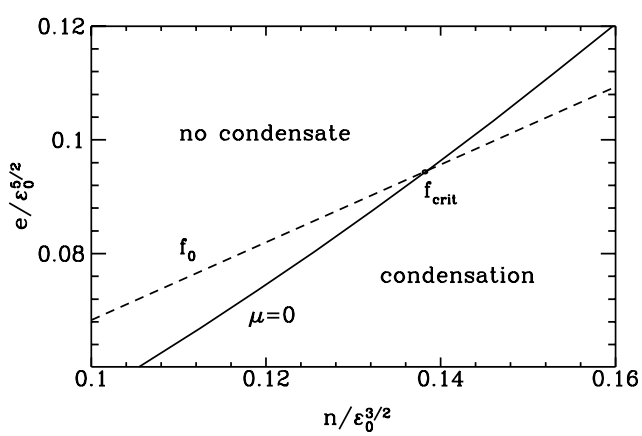

FIG. 3. The phase plane of the system. Below the solid line $\mu = 0$ the condensate is non-zero in equilibrium. The dashed line corresponds to the variation of the parameter f_0.

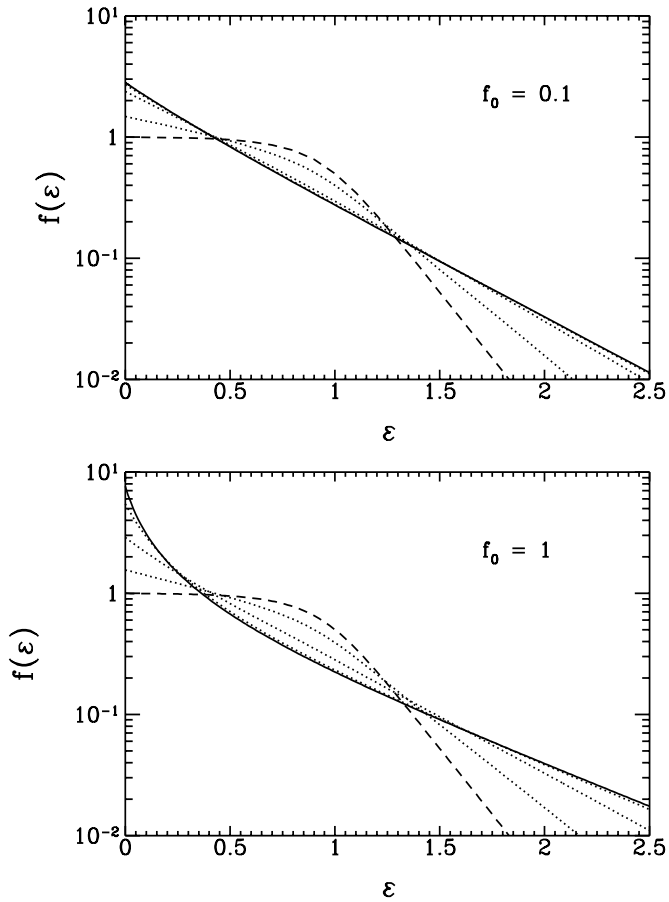

FIG. 4. Snapshots of the distribution function in non-condensate case. The dashed line corresponds to the initial distribution; the equilibrium distribution is presented by the solid curve; dotted curves correspond to the results of numerical integration at different moments of time $\tau = 1, 5, 10, 20$.

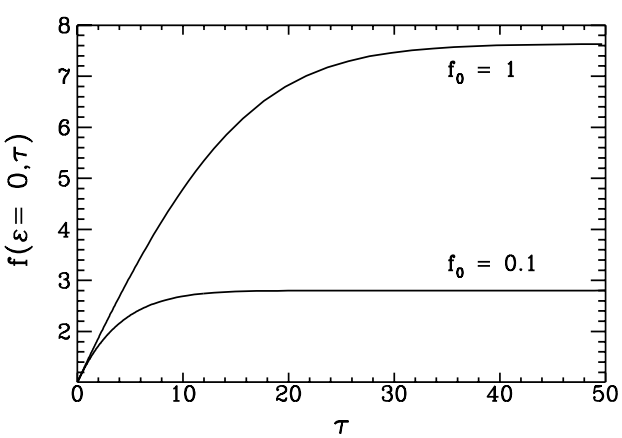

FIG. 5. The distribution function at zero energy as a function of time for two cases presented in Fig. 4.

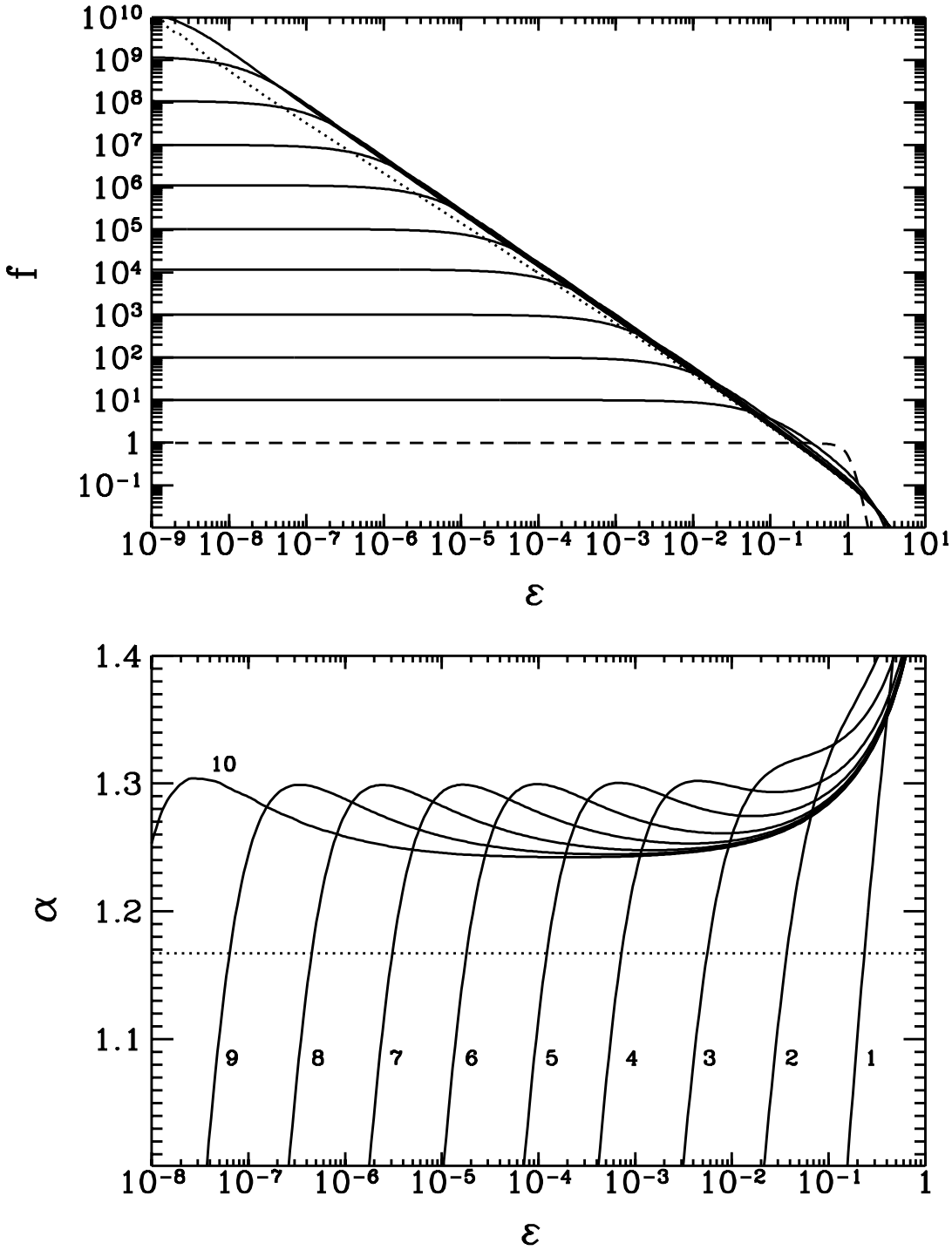

FIG. 6. The distribution function of self-interacting bosons (top) and its logarithmic derivative (bottom) are shown at different moments of time prior to condensate formation. The dashed line is the initial distribution; the dotted line corresponds to the power law $f(\varepsilon) \propto \varepsilon^{-7/6}$.

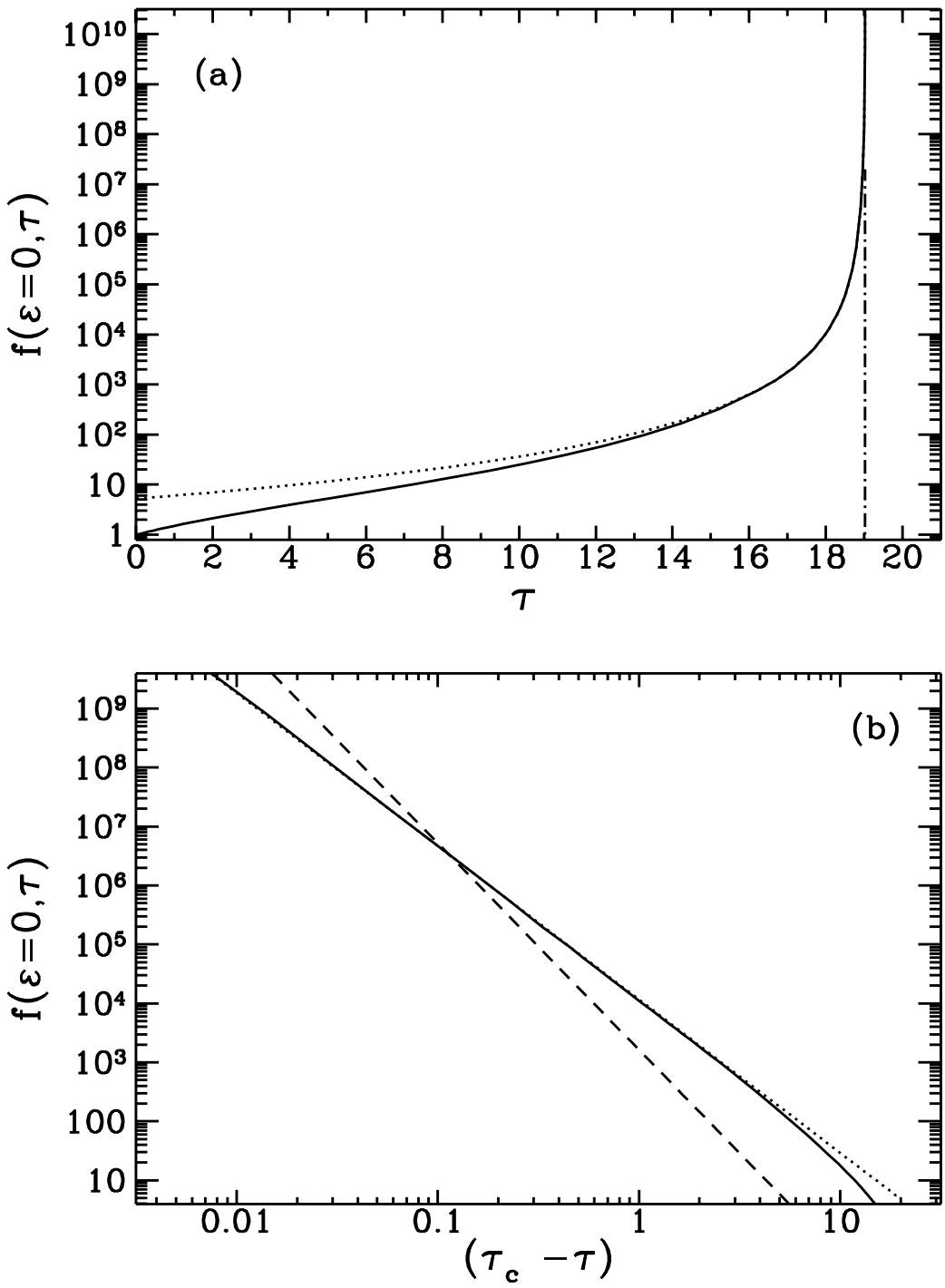

FIG. 7. The distribution function at $\varepsilon = 0$ for the case presented in Fig. 6 (the solid curves). The dotted curve in both figures is a solution to self-similarity equations, $f \propto (\tau_c - \tau)^{-2.6}$, which was found with $\alpha = 1.24$, see Section V. The dashed line in Fig. (b) is the power law $f \propto (\tau_c - \tau)^{-3.5}$ which would correspond to $\alpha = 7/6$.

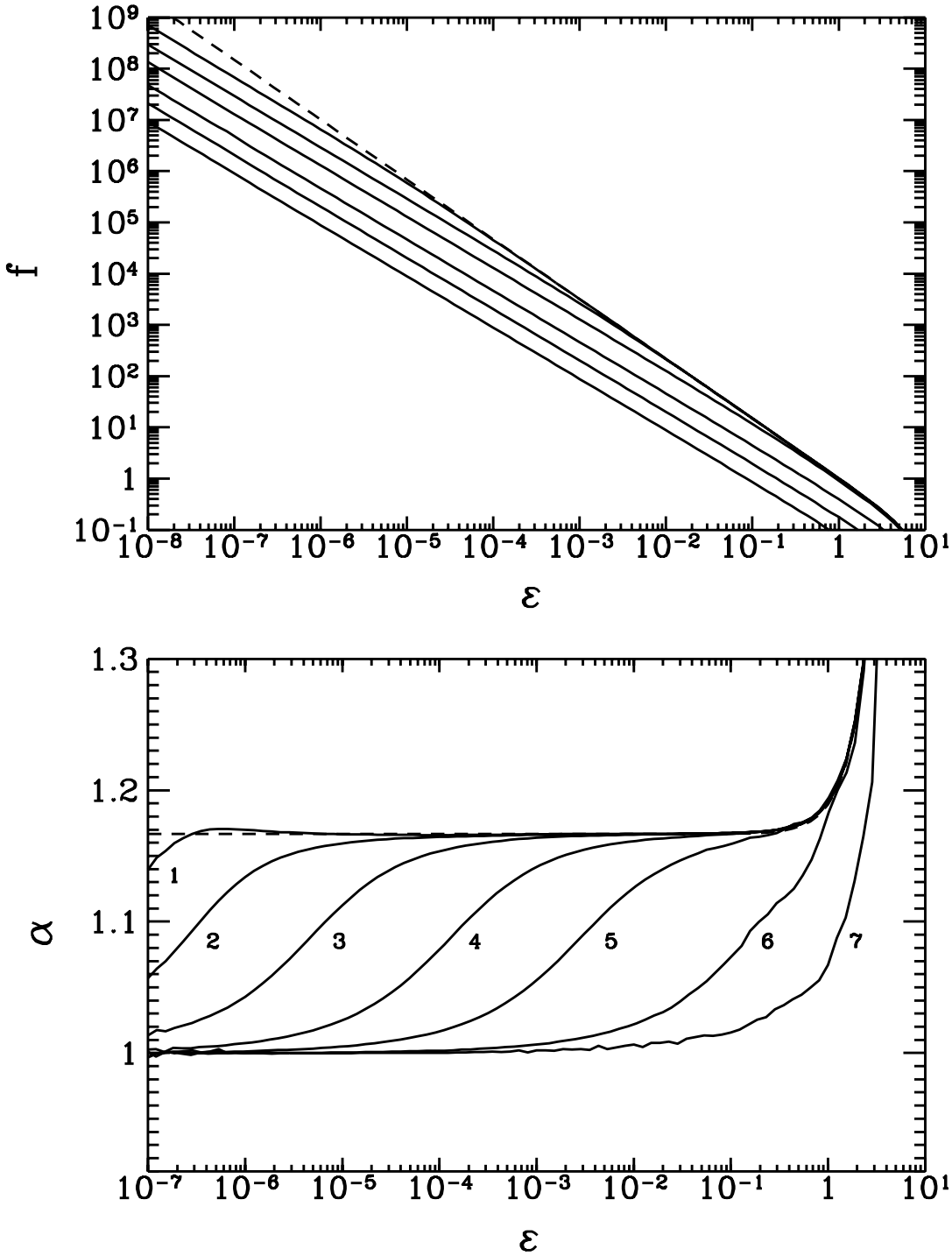

FIG. 8. The distribution function of self-interacting bosons (top) and its logarithmic derivative (bottom) are shown at different moments of time during condensation. The dashed line is the initial distribution.

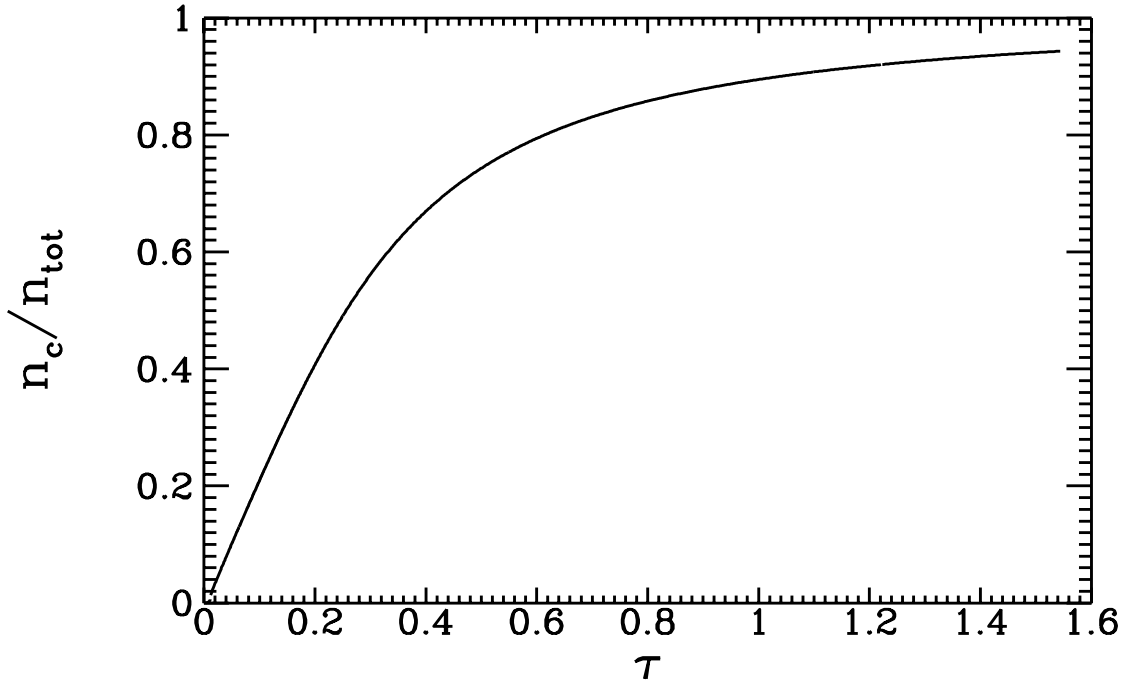

FIG. 9. Fraction of condensed particles as a function of time for the case presented in Fig. 8.

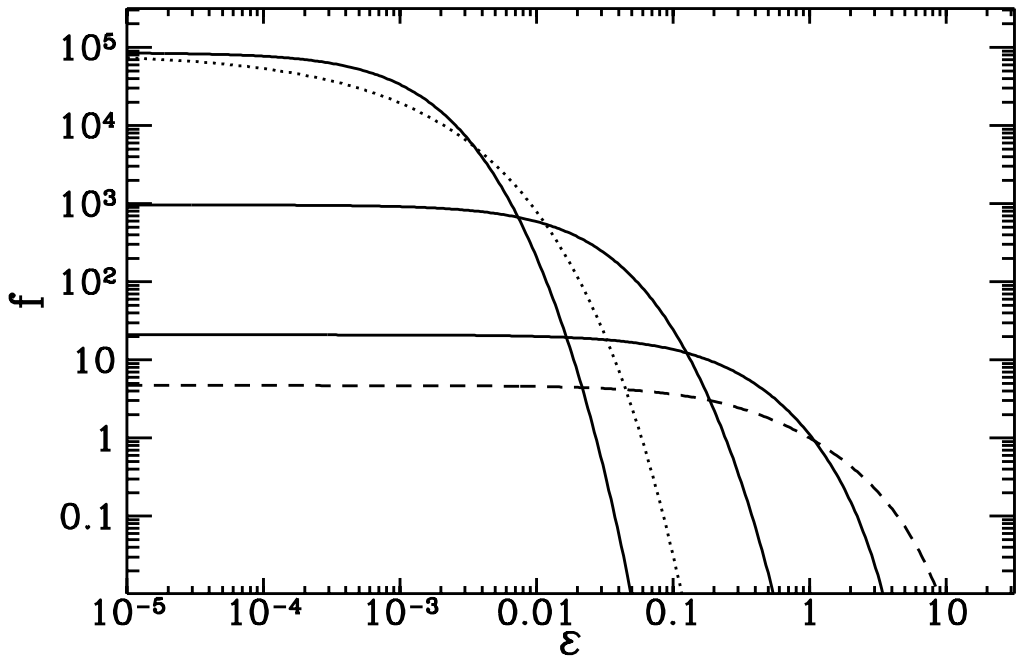

FIG. 10. The distribution function of bosons interacting with the cold gas of fermions is shown at different moments of time by the solid curves. The dashed curve is the initial distribution, the dotted curve corresponds to the Fokker-Planck approximation of Ref. [13].

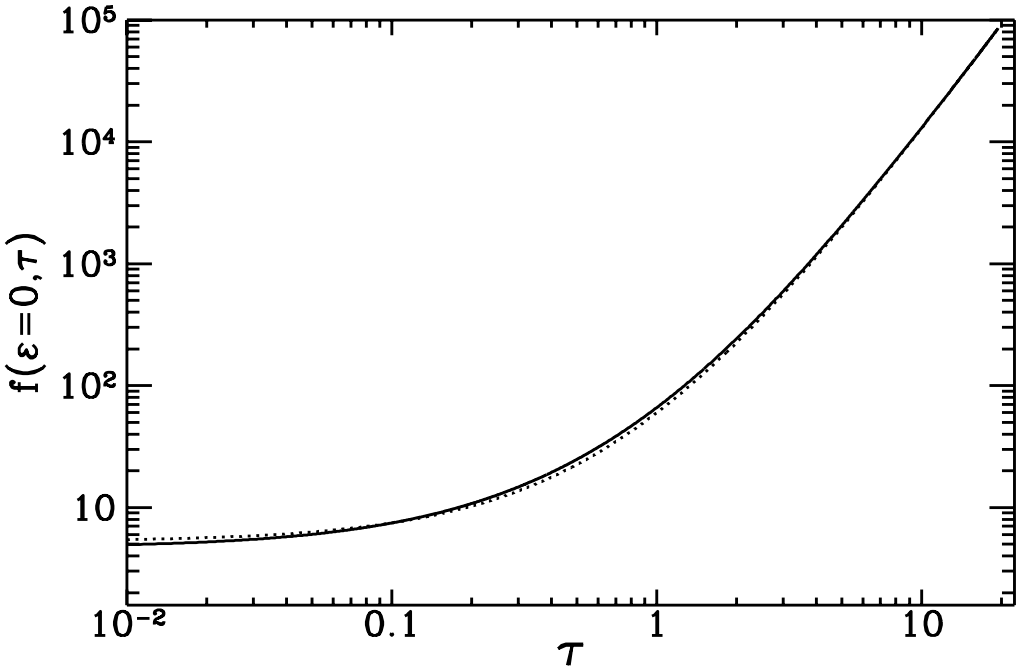

FIG. 11. The distribution function at $\varepsilon = 0$ for the case presented in Fig. 10. The dotted line is the power low $f \propto (\tau + \tau_0)^3$, which is a solution to self-similarity equations, see Section V.